



Universiteit
Leiden
The Netherlands

Ruthenium-peptide conjugates for targeted phototherapy

Zhang, I.

Citation

Zhang, I. (2023, July 4). *Ruthenium-peptide conjugates for targeted phototherapy*. Retrieved from <https://hdl.handle.net/1887/3628436>

Version: Publisher's Version

License: [Licence agreement concerning inclusion of doctoral thesis in the Institutional Repository of the University of Leiden](#)

Downloaded from: <https://hdl.handle.net/1887/3628436>

Note: To cite this publication please use the final published version (if applicable).

1

Introduction

1.1 Metalldrugs

As leading cause of death worldwide, cancer is responsible for nearly 10 million deaths in 2020 according to World Health Organization (WHO).¹ Currently, cancer patients are mainly treated with surgery, radiotherapy, and/or systemic therapy (chemotherapy, hormonal treatments, targeted biological therapies) to eliminate tumors. In the case of chemotherapy, strongly toxic chemotherapeutics such as doxorubicin (DOX), paclitaxel, 7-ethyl-10-hydroxycamptothecin (SN-38), S-crizotinib, gemcitabine, or cisplatin, are widely used.^{2, 3} Since cisplatin has been approved for the treatment of cancer in the clinics in 1978, metalldrugs have become an important line of research in oncology. Figure 1.1a shows the chemical structure of cisplatin and some of its derivatives that have been approved for clinical use worldwide or regionally.⁴ ⁵ As shown in Figure 1.1b, the predominate cell-killing mechanism of cisplatin is based on three steps: (i) cellular uptake by passive diffusion, or with the help of an active transporter such as the copper transporter 1 (CTR1), (ii) hydrolysis of the chloride ligand(s) and formation of a mono or bis-aqua intermediate, and (iii) binding of the intermediate aqua complexes to DNA *via* coordination to N7 of the purine bases.⁶ Upon DNA platination, DNA repair is prevented. Cisplatin treatment leads hence to DNA damage, which subsequently triggers apoptosis of the cancer cells. However, many tumor cells exhibit some degree of resistance against cisplatin treatment, for example *via* increased DNA repair, inefficient intracellular accumulation, or cytosolic inactivation by overexpression of glutathione, metallothionines or further cytoplasmic, nucleophilic scavengers. Mutations that increase these effects limit the performance of platinum anticancer drugs. In addition, these drugs are also characterized by a range of severe side effects, including nausea, nephrotoxicity, cardiotoxicity, hepatotoxicity and neurotoxicity, which limits the treatment efficacy.⁷

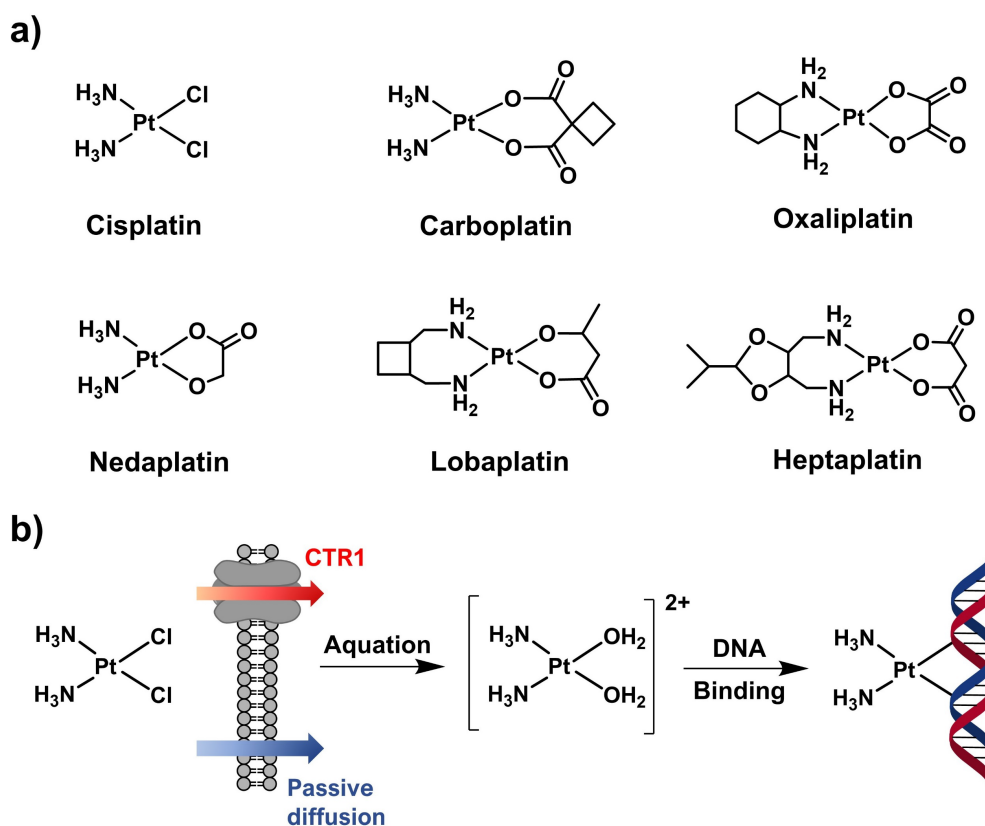


Figure 1.1. (a) Chemical structures of platinum-based anticancer drugs approved for clinical use worldwide or regionally. (b) Scheme representing the mode-of-action of cisplatin as DNA-targeted anticancer drug.

The resistance to and side effects of platinum-based anticancer drugs observed in the clinics have brought the needs for novel metal-based anticancer drugs with better performance. In the past decades, researchers have looked for anti-tumor compounds based on alternative metals such as Au,⁸ Pd,⁹ Fe,¹⁰ Ru,¹¹ and Ir,¹² of which some have been approved or are currently in clinical trials (Figure 1.2). Among these alternative drugs, ruthenium(II) polypyridyl complexes have been the focus of intense investigations due to their appealing chemical and photochemical properties. Three Ru(III) complexes (NAMI-A, KP1339 and BOLD-100) and one photoactivatable ruthenium(II) polypyridyl complex (TLD1433) (Figure 1.2) have progressed to clinical trials. Such complexes typically absorb visible light (metal-to-ligand charge transfer (MLCT) band \approx 400-550 nm) and possess long-lived triplet excited states. Many of them emit light in the red or near-infrared (NIR) region of the spectrum ($\lambda_{em} \approx$ 580-800 nm).^{13, 14} These photochemical properties have made such complexes attractive in photo-based anticancer therapy, a class of treatment modalities in which the therapeutic action of a drug can be tuned (or switched on) by light irradiation of the tumor. Interestingly, the photophysical and chemical

properties of ruthenium(II) polypyridyl complexes can be fine-tuned by altering the nature and the structure of the polypyridyl ligands bound to the ruthenium(II) center. For example, complexes can be designed that can either emit light from their triplet excited state (phosphorescence), transfer energy or electrons, or perform photosubstitution reactions, using relatively simple chemical principles.^{15, 16} Furthermore, due to the octahedral geometry of most of these complexes, chemists can play with their 3-dimensional architecture or modify functional groups on the ligands to fine-tune their biological properties and in order to bind them selectively to biomolecular targets.^{17, 18}

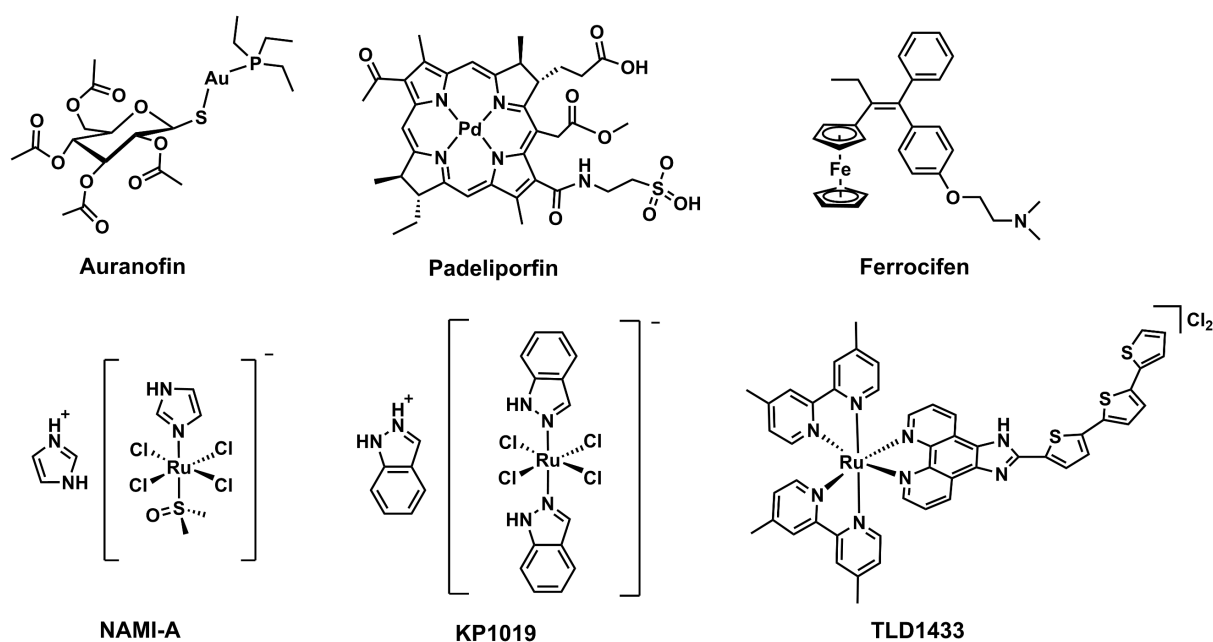


Figure 1.2. Chemical structures of non-platinum, transition metal-based anticancer compounds currently approved or in clinical trials.^{8, 9, 11}

1.2 Anticancer phototherapy

The therapeutic use of light in modern medicine originated from the Nobel prize-winning work of Finsen on the treatment of lupus vulgaris with UV light in 1896.¹⁹ The considerable advance represented by phototherapy is that it allows clinicians to administer a prodrug that disperses throughout the body with limited effects and toxicity, while upon local light activation the prodrug is activated and become highly toxic only in the irradiated area. This spatial and temporal activation can significantly reduce collateral damage to non-irradiated areas, particularly in the case of cancer therapy, in which the side effects to patients is controllable. Besides the discovery of new generations of light-activatable drugs, the physical and technological progress of light sources and light-delivery technologies (such as fiber optic light guides) over the last decades has made this therapeutic method very versatile.²⁰ Next to

treatments of tumors at an available surface of the body (skin, esophagus, bladder, lungs), light irradiation of internal organs is also possible nowadays. Currently, the related clinical trials for cancer treatment of the brain, pancreas, liver, and prostate are ongoing as well.²¹

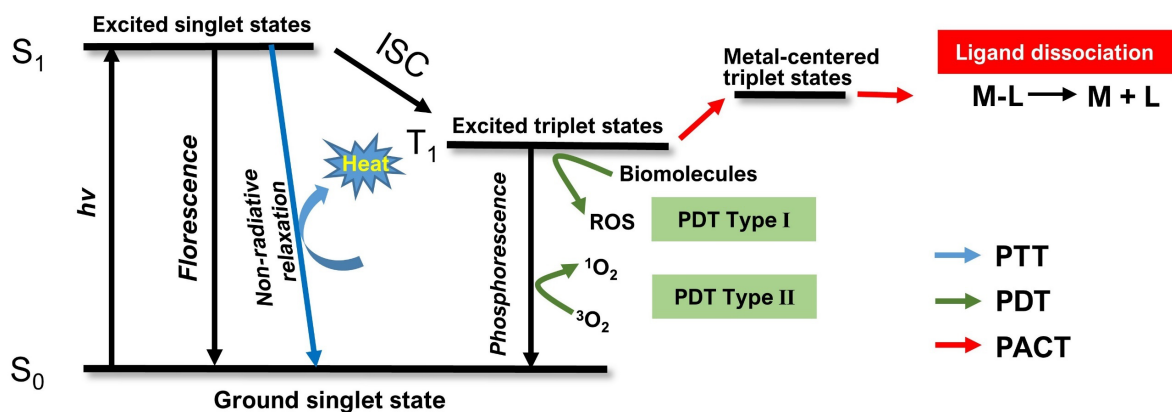


Figure 1.3. A modified Jablonski diagram of PTT (blue arrow), PDT (green arrow) and PACT (red arrow) pathway.²²⁻²⁴

Hitherto, anticancer phototherapy entails mainly three different pathways: photothermal therapy (PTT), photodynamic therapy (PDT), and photoactivated chemotherapy (PACT). Unlike PTT, causing thermal damage of the irradiated cancer cells, the toxicity in PDT and PACT arises from the light-induced formation of chemical toxins. Depending on the photochemical activation pathway, the photoactivated agents may have different modes-of-action in a cancer cell (Figure 1.3). PTT agents absorb light energy and evolve from a ground state to an excited singlet state S_1 . The electronic excitation energy then undergoes vibrational relaxation, a non-radiative form of excited state decay, and returns to the ground state which is mediated by collisions between the excited agent and the surrounding molecules. Consequently, increased kinetic energy leads to heating of the tumor microenvironment, and localized thermal damage occurs.²⁵ Similar to PTT, PDT and PACT agents first generate an excited singlet state upon absorption of a photon with the required energy. After intersystem crossing (ISC), however, these singlet states transform into relatively long-lived triplet excited states T_1 . For PDT prodrugs, so-called photosensitizers, the molecule in its lowest triplet (T_1) excited state can either return to the ground state through phosphorescence, or interact with surrounding molecules *via* electron transfer or energy transfer. Two mechanisms of reactive oxygen species (ROS) generation can be considered, namely PDT type I and PDT type II (Figure 1.3).²⁶ In PDT type I, the photosensitizer in the triplet excited state reacts with biomolecules or O_2 through electron transfer with the productions of superoxide anions ($O_2^{\cdot-}$), dihydrogen peroxide (H_2O_2), or hydroxyl radicals (OH^{\cdot}). In PDT type II, the photosensitizer transfers energy to triplet

ground-state molecular oxygen ($^3\text{O}_2$) to generate highly reactive singlet oxygen ($^1\text{O}_2$). This mechanism is considered to be the primary mode of action for most approved PDT agents used in the clinics so far. Whether from PDT type I or type II, the ROS produced photochemically in PDT react further with biomolecules, which causes chemical damage in the irradiated area, ultimately leads to cell death.²⁷⁻²⁹ As note, type I and type II mechanisms sometimes occur simultaneously in PDT.¹⁸

In PACT the excited state decays *via* rupture of a chemical bond. For PACT agents built from a ruthenium(II) center and a set of polypyridyl ligands, ISC to T_1 occurs within <100 fs due to the strong heavy-atom effect of ruthenium. Usually, this T_1 state has a metal-to-ligand charge transfer character ($^3\text{MLCT}$), and can lead either to phosphorescence, ROS generation (PDT), or non-radiative decay (PTT). Albeit, a sub-set of ruthenium polypyridyl complexes also possesses a metal-centered triplet state (^3MC , also called ^3LF state for “ligand-field” state) proximate to the $^3\text{MLCT}$ state. In such a case, thermal promotion of the $^3\text{MLCT}$ to the ^3MC state leads to elongation of a ruthenium-ligand bond distance, resulting in cleavage of the ligand from the metal center and photosubstituted by solvent molecules. This “uncaging” process generates two photoproducts, i.e., the dissociated ligand and an “uncaged” metal complex, both of which are intended, individually or in combination, be more toxic than the starting prodrug.³⁰ Despite of in PTT and PDT the drug stays in their initial configuration during photoactivation and turnover catalytically, the composition of PACT complexes changes upon light irradiation. A pivotal difference between these three pathways is the high dependence of the effectiveness of PDT in the presence O_2 , as a consequence of its mode of action. Nevertheless, low O_2 concentrations are often observed in solid tumors due to the rapid consumption of O_2 accompanying highly proliferating cancer cells, and to inadequate O_2 delivery. In fact, so-called hypoxia is sometimes considered as a characteristic hallmark of cancer.³¹ For example, the dioxygen pressure ($p\text{O}_2$) in brain tumors lies around 5 mmHg while that in normal tissue is nearly 50 mmHg.³² Hypoxia condition is one of the most significant barriers for the use of PDT so far. One vision for PACT is that its independence from the presence of O_2 may help solving this problem, enabling the treatment of tumors that are hypoxic.

1.3 Ruthenium-based PDT and PACT

Many phototherapeutic compounds are ruthenium(II) polypyridyl complexes, working either *via* a PDT or a PACT pathway. Figure 1.4 illustrates different ruthenium complexes that are active *via* the PDT pathway (Figure 1.4a), the PACT pathway (Figure 1.4b), or in a dual PDT+PACT pathway (Figure 1.4c). In fact, to some extent it is possible to connect the

phototoxicity pathway of a ruthenium complex to its chemical structure. TLD-1433 (**Ru1**) is a representative PDT complex developed by the group of McFarland; it was also the first Ru(II)-based photosensitizer entering human clinical trial (ClinicalTrials.gov, identifier NCT03053635).³³ It shows $^1\text{O}_2$ generation quantum yields near unity,³⁴ and is activated by green (520 nm) or red light (625 nm). Upon red light activation (625 nm, light dose: 100 J/cm²), Its EC₅₀ value (defined as the concentration that kills half of a cell population, compared to untreated cells) towards HL-60 human leukemia cells is around $7.20 \pm 1.0 \mu\text{M}$, while its toxicity in the dark is much lower (EC₅₀>300 μM).³³

A series of ruthenium(II)-arene complexes $[\text{Ru}(\eta^6\text{-arene})(\text{L})(\text{X})]^{n+}$, in which X is a monodentate ligand (usually a halide) and L comprises neutral monodentate or chelating ligands, has been widely studied as PACT complexes.³⁵⁻³⁷ The anticancer activity of this type of complexes is associated with the labile nature of the X⁻ ligand. Replacement of X⁻ by pyridines may render the anticancer compound light-sensitive. As an example, $[\text{Ru}(\eta^6\text{-}p\text{-cymene})(\text{bpm})(\text{py})]^{2+}$ (**Ru4**, bpm = 2,2'-bipyrimidine, py = pyridine) designed by the Sadler group, undergoes pyridine dissociation and DNA binding upon irradiation with white light (400-600 nm), showing PACT potential.³⁵

Our group has also developed a series of PACT ruthenium complexes, the therapeutic activity of which either relies on the toxicity of the dissociated ligand,^{38, 39} or on that of the uncaged metal center.^{40, 41} For example, in the microtubule-targeted compound $[\text{Ru}(\text{tpy})(\text{bpy})(\text{MTI})](\text{PF}_6)_2$ (**Ru5**, tpy = 2,2';6'-2''-terpyridine; bpy = 2,2'-bipyridine), the toxic microtubule-targeted inhibitor (MTI) is “caged” by the ruthenium-polypyridine complex $[\text{Ru}(\text{tpy})(\text{bpy})]^{2+}$ moiety in the dark. After light activation, MTI is liberated and inhibits tubulin polymerization in cancer cells.³⁹ This “photocaging” strategy was also applied to other ligands,^{38, 42, 43} such as the cytotoxic nicotinamide phosphoribosyltransferase (NAMPT) and Glut-1 enzyme inhibitor STF31. Alternatively, the metal-containing photoproduct might be the cytotoxic species. For example, the bis-aqua ruthenium-based photoproduct of $[\text{Ru}(\text{Ph}_2\text{phen})_2(\text{mtmp})]\text{Cl}_2$ (**Ru6**, Ph₂phen = 4,7-diphenyl-1,10-phenanthroline; mtmp = 2-methylthiomethylpyridine), showed high toxicity (EC_{50,light} = 0.48 μM) towards human lung cancer cell line A549, while when the non-toxic mtmp caging ligand still bounded, the complex was less toxic (EC_{50,dark}=2.66 μM).

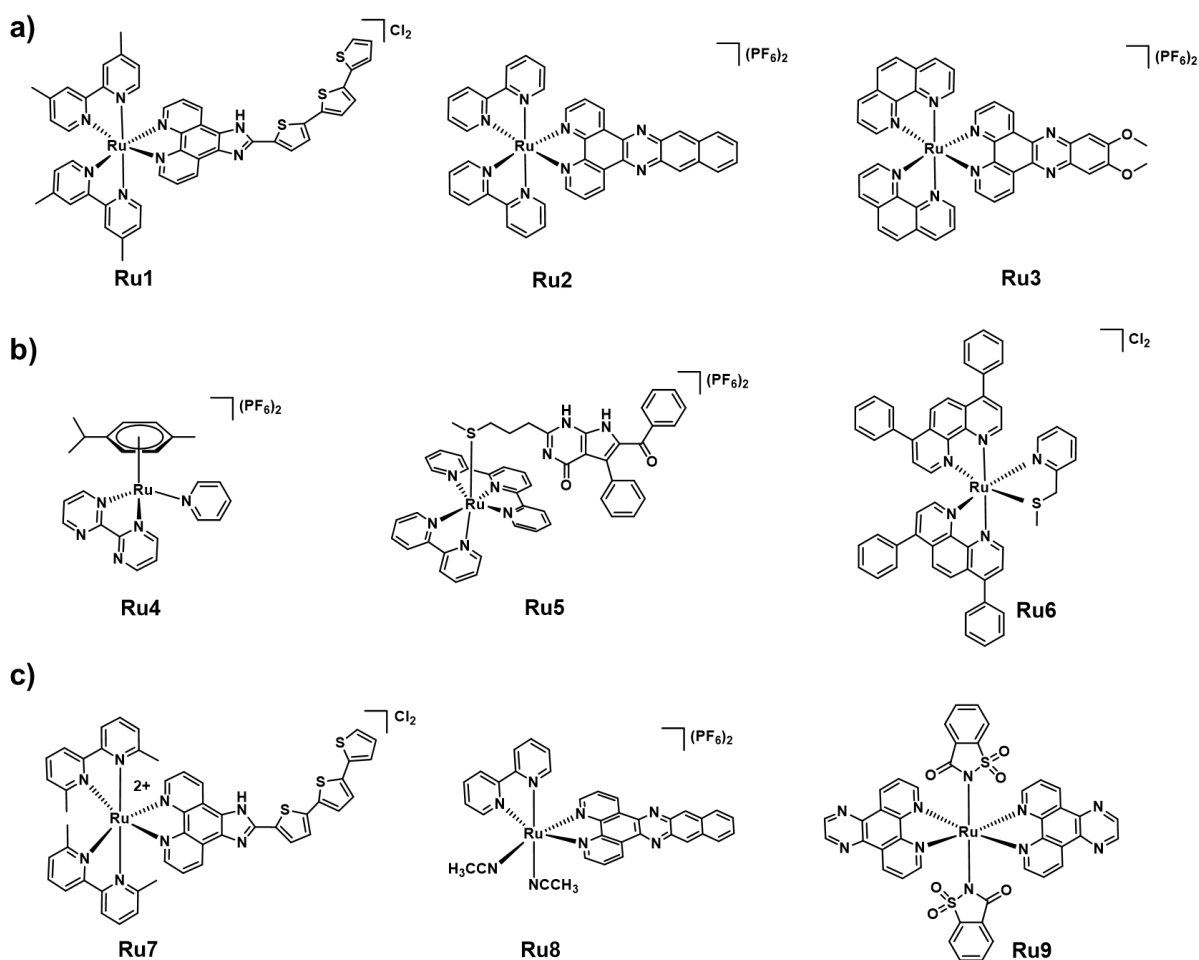


Figure 1.4. Examples of ruthenium(II) polypyridine complexes used as PDT drug (a)^{33, 44, 45}, PACT drugs (b),^{35, 39, 41} or dual PDT+PACT drug (c).⁴⁶⁻⁴⁸

Apart from the development of anticancer ruthenium-based compounds for PDT or PACT, other attempts aimed at making molecules exhibiting synergetic phototherapeutic effects combining a PDT and a PACT effect. In fact, transformation of a PDT compound to a PACT compound can be accomplished by lowering the relative energy of the ^3MC state, compared to the $^3\text{MLCT}$ state, facilitating thermal promotion to the ^3MC dissociative state from the $^3\text{MLCT}$ state. If the ^3MC state is at an intermediate energy level, both $^1\text{O}_2$ generation and photosubstitution can be obtained simultaneously. A strategy to attain this effect is the use labile ligands, for example, thioethers RSR' (i.e. **Ru6**) or nitriles NCR (as in **Ru8**). These ligands are weaker σ -donors than (poly)pyridine ligands,⁴⁹ which can lower the ^3MC state and promotes photosubstitution.

Another method to stimulate photosubstitution is to use ligands that distort the 1st coordination sphere of the metal center,⁴⁶ such as 2,2'-biquinoline (biq),^{38, 50} 2,2';6',2''-terpyridine (tpy),^{39, 51} or 6,6'-dimethyl-2,2'-bipyridine (dmb).^{38, 52, 53} Complexes bearing these ligands often show

PACT properties, while non-distorted analogues are often active *via* a PDT mechanism. Figure 1.5a displays the comparison of structure and mode of action between TLD-1433 and its distorted analogue during light activation. As mentioned above, the PDT complex TLD-1433 (**Ru1**) has a $^1\text{O}_2$ generation quantum yield near unity and does not undergo any photosubstitution reaction. Shifting the position of the methyl groups on the chelating ligand from *para* (4,4'-dimethyl-2,2'-bipyridine = 4,4'-dmb) to the *ortho*-position towards nitrogen atoms in the pyridine, the complex $[\text{Ru}(6,6'\text{-dmb})_2(\text{IP-3T})]\text{Cl}_2$ (**Ru7**, Figure 1.5b) is obtained, which photoreleases one of the 6,6'-dmb chelating ligands by a rapid photosubstitution process. At the same time, owing to the low-lying π orbitals on the tris-thiophene (3T) fragment, high $^1\text{O}_2$ generation quantum yields were retained ($\Phi_{\Delta}=0.42$),⁵⁴ so that **Ru7** works both *via* PACT and PDT mechanisms, resulting in particularly high anticancer efficiency (photo index (PI, $\text{EC}_{50,\text{dark}}/\text{EC}_{50,\text{light}} > 700$)).⁴⁶

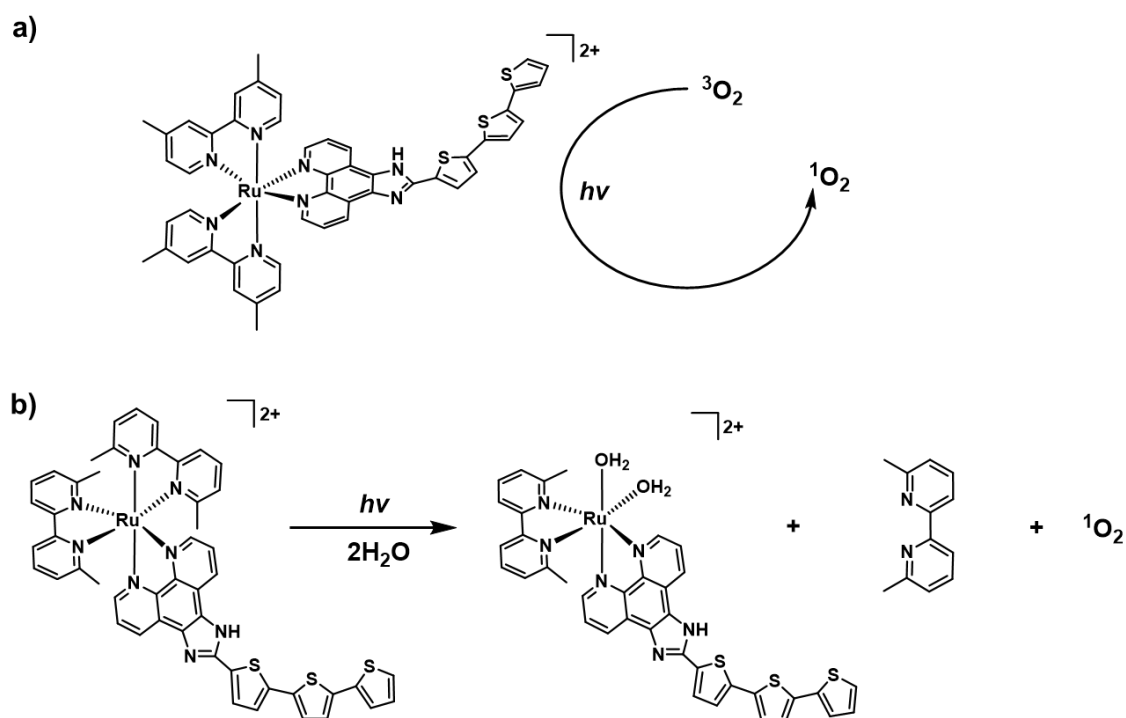


Figure 1.5. Formula and activation mode of the PDT complex TLD1433 (a) and of its analogue $[\text{Ru}(6,6'\text{-dmb})_2(\text{IP-3T})]\text{Cl}_2$ (b) which is working as a dual PDT and PACT complex upon light activation.

Noticeably, a synergistic effect of PDT with chemotherapy can improve the anticancer efficiency of both.^{55, 56} Chemotherapy may improve the sensitivity of the cancer cells to ROS generated by PDT, while the ROS generated by PDT may suppress the drug-efflux activity that limits the efficacy of chemotherapy. The light-activated character of such molecules makes

combined treatment more controllable.²² For example, a synergetic treatment by Doxorubicin with PDT therapy (Hematoporphyrin derivative (HPD) + 630 nm red light) was shown to suppress the tumor growth in mice more effectively than PDT or Doxorubicin alone.⁵⁷ Thus, complexes with both PDT and PACT effects may result in synergism, leading to an important direction for the development of ruthenium-based anticancer drugs.

1.4 Peptide conjugation to ruthenium complexes

Besides the physical selectivity of phototherapy, as local irradiation results in spatially-resolved delivery of the toxicity, several issues still need to be addressed for enhancing the activity and selectivity of metallodrugs towards tumors (cell type, intracellular, molecular, physiological area, etc.), and for increasing their biocompatibility.⁵⁸ In order to increase the biological selectivity of a (pro)drug and thus lower its side effects, one strategy has shown great promise: the conjugation of the ruthenium drug to tumor-targeting molecules,¹⁸ which interact efficiently *via* non-covalent interactions with proteins that are overexpressed in tumor cells. As shown in Figure 1.6a, researchers have conjugated different kinds of tumor-targeting biomolecules to metallodrugs, such as peptides,^{59,60} peptoids,⁶¹ antibodies,^{62,63} or proteins.^{63,64} These functional groups can target e.g. cell adhesion proteins,⁶⁵ organelles,^{66,67} growth factors,^{61,68} or G-protein-coupled receptors.^{59,69} In particular, the use of peptides has drawn great attention as their easy synthesis, low toxicity, and high biological specificity. Peptides are defined as short sequences of 2-50 amino acids connected to each other through amide bonds; they often represent a minimal functional unit retained from proteins. Technological developments have led to large libraries of natural and synthetic peptides, advanced peptide candidates can be selected *via* high throughput screening campaigns.⁷⁰ Last but not least, each amino acid residue in a peptide can be modified at will, adjusted and replaced by multiple auxiliary molecules, which allows researchers to attach various functional groups such as fluorophores,⁷¹ proteins,⁷² or Poly(ethylene glycol) (PEG) groups,⁷³ and other groups.⁷⁴⁻⁷⁶

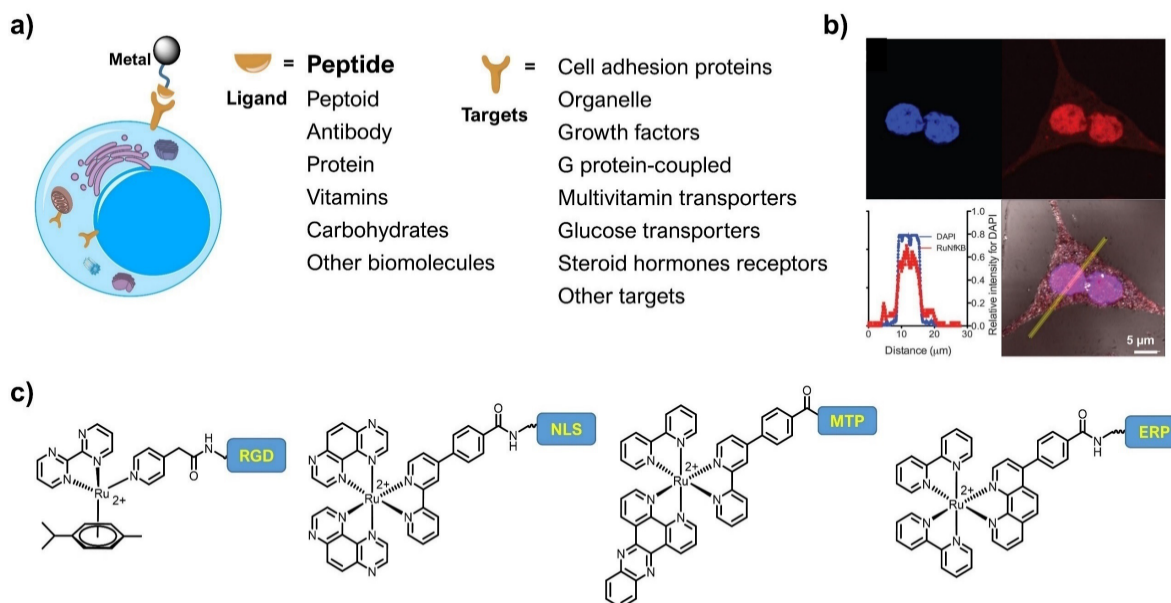


Figure 1.6. (a) Schematic representation of anticancer metal complexes incorporating a tumor-targeting ligand for active targeting of cancer cells. (b) An emissive Ru(II) polypyridyl complex conjugated with nuclear location signal peptide (NLS) shows efficient nuclear accumulation in CHO cells.⁷⁷ (c) Examples of Ru-peptide conjugates targeting integrins (sequence: RGD-NH₂), nuclei (NLS sequence: VQRKRQKLMR-NH₂), mitochondria (MTP = mitochondria-targeting peptide, sequence: FrFKFrFK-NH₂, r represents D-Arg), or endoplasmic reticulum (ERP = endoplasmic reticulum peptide, sequence: RQIKIWFQNRRMKWKK-NH₂).^{37, 67, 78, 79}

Peptide conjugation to ruthenium(II) polypyridyl complexes has been used effectively to improve water solubility, enhance cellular uptake, act as active tumor targeting motifs, and improve biocompatibility, that altogether contributes reducing systemic toxicity (Figure 1.6).⁸⁰ It is particularly attractive to use a peptide that can bind to biological markers overexpressed on the surface of tumor cells to increase the tumor accumulation efficacy of a complex. For example, an adhesion-protein family called integrin, which mainly locates on plasma membranes, were proved to be associated with many cancer-related hallmarks such as adhesion and signaling.⁸¹ Integrins are divalent cation-dependent heterodimeric membrane glycoproteins composed of non-covalently associated α - and β -subunits. There are 18 α - and 8 β -subunit integrins in mammals, which combine into 24 subtypes of integrin heterodimers.⁸² Each subunit is composed of (i) an extracellular domain, (ii) a single transmembrane region, and (iii) a cytoplasmic region.⁸³ Typically, ligand binding can be realized through the recognition of a small peptide sequence that is derived from classical extracellular matrix proteins, including fibronectin, fibrinogen, vitronectin, osteopontin, and several other adhesive extracellular matrix

proteins.⁸⁴ As representative, the tripeptide sequence arginyl-glycyl-aspartic acid (RGD) was proved to bind with several integrin heterodimers (Figure 1.7a). Based on this observation, many RGD-conjugated bioactive compounds have been developed for preferential binding to e.g. integrin $\alpha_v\beta_3$.⁸⁵ Figure 1.7b shows the binding modes of the linear RGD peptide with two integrin examples, i.e. $\alpha_v\beta_3$ and $\alpha_{IIb}\beta_3$. The two charged residues Asp and Arg are key factors for the specific recognition of the RGD peptide with integrin: they allow for coordination of divalent metal ions (i.e. Asp with β_3 metal ion-dependent adhesion site (MIDAS)) and the formation of salt-bridge hydrogen bonds (i.e. Arg with Asp218 of α_v), respectively.^{86, 87} The binding of the RGD sequence to integrins is strongly influenced by the rigidity of their conformation. For example, cyclic RGD peptides show improved binding affinity and also possess higher plasma stability.⁸⁸ Most promisingly, overexpression of the related integrin subunit have been repeatedly reported in cancer cell lines, though at diverse degrees (Figure 1.7c). Thus, tumor cells with highly expressed integrin receptors have become potential therapeutic targets in oncology, and many large and small-molecule inhibitors (RGD or non-RGD containing) targeted to RGD integrin are in preclinical or clinical trials.⁸⁹

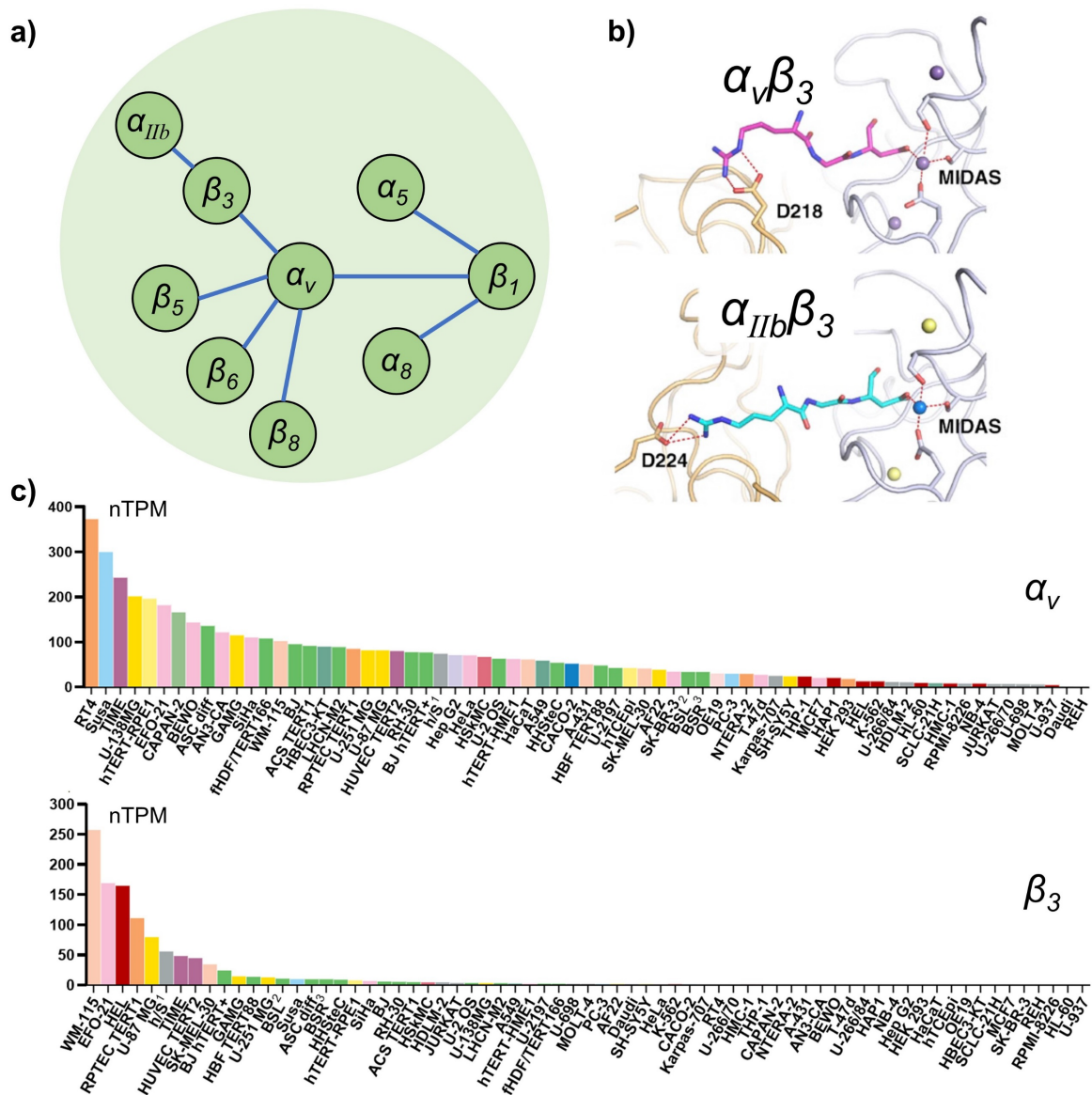


Figure 1.7. (a) Integrin heterodimeric α/β partners which are RGD receptors. (b) Illustration of the binding modes of integrin $\alpha_v\beta_3$ and $\alpha_{IIb}\beta_3$ with the RGD linear tripeptide. For the $\alpha_v\beta_3$ -RGD complex structure, the Arg of RGD is hydrogen bonded to α_v D218 from the side, and the Asp carboxylate directly coordinates the β_3 metal ion-dependent adhesion site (MIDAS) Mg^{2+} ,⁹⁰ whereas in the $\alpha_{IIb}\beta_3$ -RGD complex, Arg is hydrogen bonded to α_{IIb} D224 with head on,⁹¹ and Asp recapitulating the RGD-binding mode found in β_3 integrins. Figure is adapted from reference.⁸⁷ (c) RNA expression levels related to integrin subunit α_v and β_3 in different cancer cell lines. Figure was taken from the Human Protein Atlas (www.proteinatlas.org).^a

^a Long cell line name is simplified, **h/S**¹: hTEC / SVTERT24-B; **BSL**²: BJ hTERT + SV40 Large T+; **BSR**³: BJ hTERT + SV40 Large T + RasG12V.

1.5 Chirality in ruthenium complexes

Octahedral ruthenium (II) complexes with three bidentate ligands are chiral by virtue of the configuration of the chelating ligands around the metal center, as shown in Figure 1.8a. This results in the formation of either a left-handed Λ -enantiomer or a right-handed Δ -enantiomer.¹⁸ Like for organic structures, the two enantiomers of a (pro)drug based on chiral inorganic compounds may behave differently in biological systems due to the chiral nature of most biopolymers (nucleic acids and proteins). Thus, the two enantiomers should better be separated and studied individually.

The separation of ruthenium-centered chiral stereoisomers can be performed using different methods. For example, capillary electrophoresis (CE) has been successfully applied to separate Ru-based enantiomers,⁹²⁻⁹⁴ but this technique is limited to analytical scales. HPLC has also been used for successful separation of Ru enantiomers, using chiral stationary phases (CSPs) such as cyclodextrin⁹⁵, teicoplanin,⁹⁶ or macrocyclic glycopeptides,^{97, 98} with high efficiency, good selectivity, and at larger scales (>10 mg). Besides the use of specialized separation equipment, chemists have also tried to use chiral auxiliaries during synthesis, to obtain chiral ruthenium complexes at a large scale and in high yield. Enantiomerically pure counter ions such as *O,O'*-dibenzoyl-*L/D*-tartrate can be used to crystallize specifically one of the enantiomers of the ruthenium complex.^{99, 100} Nevertheless, introducing enantiomerically pure chiral ligands such as *N*-acetyl-*tert*-butanesulfonamide ((*R*)-ASA)¹⁰¹ or proline¹⁰² is also possible, allowing to separate diastereoisomers before replacing the chiral auxiliary by the final target ligand.

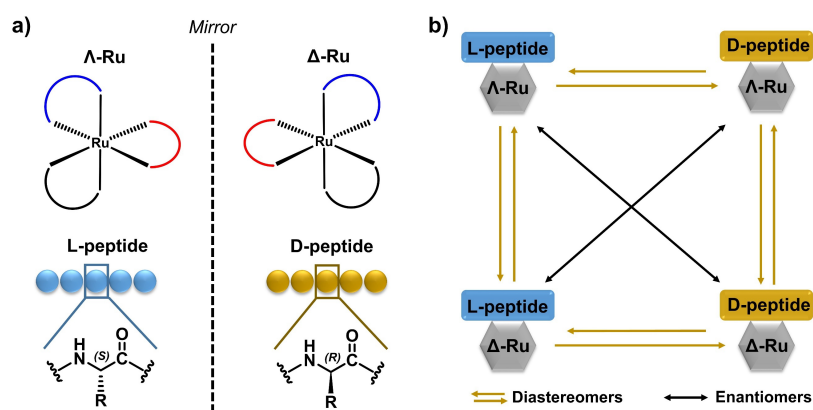


Figure 1.8. (a) The octahedral coordination geometry of three bidentate ligands bound to a Ru(II) center give a pair of chiral Λ - and Δ -enantiomers. (b) The relations between Ru-peptide isomers obtained by conjugation of a Λ -/ Δ -Ru fragment and a L-/D-peptide.^b

^b Here the peptide is fully coordinated and there is no other chiral center besides Ru.

As note, the differences in biological properties between the Λ and Δ enantiomers of a ruthenium complex are controversial. Chemical studies have shown that the two enantiomers of Ru(II) polypyridyl complexes such as $[\text{Ru}(\text{phen})_2(\text{dppz})]^{2+}$ (dppz = dipyrido[3,2-a:2',3'-c]phenazin) can interact differently with chiral biomolecules such as DNA and proteins. Dramatic differences in cellular uptake mechanism or localization have been reported, such as the Λ enantiomer of the complex $[\text{Ru}(\text{bpy})_2(p\text{-BEPIP})](\text{ClO}_4)_2$ ($p\text{-BEPIP}$ = 2-(4-phenylacetylenophenyl)-1*H*-imidazo[4,5*f*][1,10]phenanthroline]) that was mostly found in the nucleus while the Δ enantiomer was localized in the cytoplasm.¹⁰³ However, further studies have found no differences in cellular staining between another Δ and Λ enantiomers of Ru complexes.¹⁰⁴ Overall, for many examples of ruthenium complexes the Δ and Λ enantiomers are capable of distinct behavior in the chiral environment of a cell, while some maybe not.

For Ru-peptide conjugates not only the chirality of the ruthenium complexes has to be considered, but also that of the peptide, as this may also influence the biological properties of the conjugate. Natural peptides in animals and plants are composed of about 20 different types of L-amino acids since ribosomes are specific to L-amino acids. D-amino acids rarely occur in organisms and peptides containing D-amino acids are not easily digested or degraded.¹⁰⁵ Compared to all L-peptides, this property often leads to higher stability in physiological environment for peptides containing D-amino acids. For example, a D-peptide drug which is currently under clinical trial for use in Alzheimer's disease (RD2 peptide, sequence: ptlhthnrrrrr, D-type amino acids are shown by lowercase letters), was shown to possess longer half-life, higher oral bioavailability and higher resistance against metabolization, compared to the corresponding L-peptide.^{106, 107} However, the binding specificity of peptides containing D-amino acids to the natural protein targets might be suboptimal compared to L-analogues, and the side effect from this unnatural products in psychological condition should be inspected.

It is interesting to explore further the chemistry of Ru-peptide conjugates containing both Λ or Δ ruthenium enantiomers and L or D peptides. In absence of any other chiral center, we can expect four stereoisomers for each Ru-peptide conjugate, i.e., $\Lambda\text{-Ru/L-P}$, $\Delta\text{-Ru/L-P}$, $\Lambda\text{-Ru/D-P}$ and $\Delta\text{-Ru/D-P}$. They are either enantiomers or diastereomers, as shown in Figure 1.8b.

1.6 Aim and outline of this thesis

The above introduction has highlighted a few existing applications of targeting peptides for ruthenium-based phototherapy, but several questions need to be addressed.

The use of peptides for bioimaging using emissive ruthenium complexes has been proposed already, but Ru-peptide conjugates for anticancer therapy are scarce.^{58, 78, 79} So far, peptide functionalization of ruthenium complexes has been based on the covalent modification of spectator polypyridyl ligands, without direct coordination of side chains of the peptide to the metal center.^{37, 108} As long as the spectator ligand is bound to the metal, the peptide remains bound as well, and the metal center cannot escape. Otherwise, amino-acid residues such as methionine (M), histidine (H), cysteine (C), or aspartic acid (D), are known to allow for coordination of natural peptides and proteins to a metal cofactor.¹⁰⁹ The direct coordination of such amino acids to ruthenium would offer a new strategy for the conjugation of ruthenium complexes to functional proteins such as monoclonal antibodies.^{110, 111} The photochemical and photobiological properties of Ru(II) complexes are strongly related to their chemical structure, including the ligands in the 1st coordination sphere, the chirality of the ligands and of the metal center, and potentially, the amino acid sequence. To the best of our knowledge, structure-activity relationship (SAR) studies of Ru-peptide conjugates are very rare, and it is not clear whether histidines or methionines are better for making photosubstitutionally active ruthenium complexes.

In the research described in this thesis, a series of novel Ru-peptide conjugates have been developed by direct coordination of metal-binding amino acid residues in $[\text{Ru}(\text{N-N})_2(\text{peptide})]\text{Cl}_2$, where N-N are bidentate diimine spectator chelating ligands. The manuscript discusses the influence of the *N-N* ligand (Chapter 2), the chirality of the ruthenium center (Chapter 3), the peptide sequence (Chapter 4), and the chirality of the peptide (Chapter 5), on the (photo)chemical and (photo)biological properties of these conjugates, aiming for the application of such complexes to PACT treatment of cancer. An overview of the complexes described in this thesis is shown in Table 1.1.

In Chapter 2 the peptide Ac-HRGD₂-NH₂ was utilized for making Ru-peptide conjugates. Besides the central RGD sequence acting as functional motif for targeting integrin, two terminal histidine residues have been chosen to coordinate the peptide to the ruthenium center. Three different bipyridine *N-N* ligands have been used, i.e. 2,2'-bipyridine (bpy), 6,6'-dimethyl-2,2'-bipyridine (dmbpy), or 4,7-diphenyl-1,10-phenanthroline (Ph₂phen). According to the photochemical and anticancer properties of these three complexes, two of the complexes behave as PDT compounds, while the complex based on dmbpy behaves more as a PACT compound. Considering uptake, *in vitro* cytotoxicity, ROS generation, and cellular localization studies, the compound containing Ph₂phen was shown to offer the most promising properties for the

building of a phototoxic compound, and therefore was used in the research described in the other chapters of this thesis.

In the research described in **Chapter 3** the compound $[\text{Ru}(\text{Ph}_2\text{phen})_2(\text{Ac-MRGDH-NH}_2)]\text{Cl}_2$ was investigated as integrin-targeted prodrug for anticancer phototherapy. By changing the peptide of Chapter 2 into Ac-MRGDH-NH₂, i.e. by substitution of one histidine by a methionine, faster photorelease of the peptide from the Ru fragment was obtained, which turned the complex into a potential PACT compound. The peptide not only acted as a targeting motif, but also shielded the cytotoxicity of the photoproduct $[\text{Ru}(\text{Ph}_2\text{phen})_2(\text{OH}_2)_2]^{2+}$. The Λ and Δ diastereomer of $[\text{Ru}(\text{Ph}_2\text{phen})_2(\text{Ac-MRGDH-NH}_2)]\text{Cl}_2$ were separated by HPLC and compared in a broad chemical and biological study. According of which, the phototoxicity of both isomers was confirmed from a combination of a PDT and PACT pathway. The phototoxicity and tumor targeting were further confirmed not only *in vitro* but also *in vivo* using subcutaneous tumor mice models.

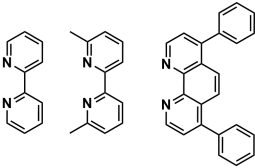
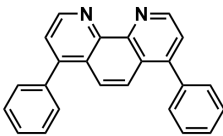
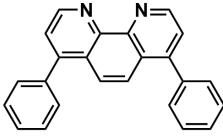
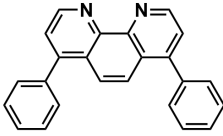
Chapter 4 comprises the consideration to use a new peptide Ac-MRGDM-NH₂ with two methionine residues for binding to ruthenium. A comparison was made between the three Ru-peptide conjugates $[\text{Ru}(\text{Ph}_2\text{phen})_2(\text{Ac-HRGDH-NH}_2)]\text{Cl}_2$ (**Ru-p(HH)**), $[\text{Ru}(\text{Ph}_2\text{phen})_2(\text{Ac-MRGDH-NH}_2)]\text{Cl}_2$ (**Ru-p(MH)**) and $[\text{Ru}(\text{Ph}_2\text{phen})_2(\text{Ac-MRGDM-NH}_2)]\text{Cl}_2$ (**Ru-p(MM)**), to understand the role of the ruthenium-binding amino acid residues on the photochemistry and photobiology of this type of conjugates. The phototoxicity mechanisms of these three conjugates were shown to be highly dependent on the nature of the coordinated amino acids. Further *in vivo* studies were realized using zebrafish embryo tumor models, in collaboration with the group of Prof. Ewa Snaar-Jagalska. The potential of this series of Ru-peptide conjugates for brain tumor therapy was demonstrated, as a result of their capability to cross the Blood Brain Barrier (BBB), to target the tumor, and to destroy it upon green light activation.

The chirality of the amino acid residues of the peptide was systematically varied for complex $[\text{Ru}(\text{Ph}_2\text{phen})_2(\text{Ac-MRGDM-NH}_2)]\text{Cl}_2$ as reported in **Chapter 5**. By conjugating three isomeric peptides Ac-MRGDM-NH₂, Ac-mrGdm-NH₂, and Ac-MrGdM-NH₂, (M, R, D are L-amino acids, m, r, d are the D-enantiomers), to the racemic compound *cis*- $[\text{Ru}(\text{Ph}_2\text{phen})_2\text{Cl}_2]$, six diastereomers Δ -[1]Cl₂, Λ -[1]Cl₂, Δ -[2]Cl₂, Λ -[2]Cl₂, Δ -[3]Cl₂ and Λ -[3]Cl₂ were successfully prepared and isolated by HPLC. Their structure, photochemistry, cytotoxicity, cellular uptake and phototoxicity mechanism were investigated and compared in detail. Upon irradiation with green light (515 nm) in water, all six diastereomers substituted their peptide for water molecules with comparatively high photosubstitution quantum yields. All diastereomers

showed considerable photoactivated cytotoxicity towards A549 cells in normoxic conditions (21% O₂, PI up to 20) and in hypoxic conditions (1% O₂, PI up to 4.5), as well as towards A549 3D tumor spheroids (PI up to >5). The limited generation of ¹O₂ and ROS confirmed that these complexes behaved mostly as PACT drugs.

In Chapter 6, a general discussion is presented of the observations reported in this thesis, as well as an outlook towards potential clinical applications of ruthenium-peptide conjugates for PACT treatment of cancer.

Table 1.1. The list of *N,N* ligand and peptides in the $[Ru(N-N)_2(peptide)]Cl_2$ conjugates reported in this thesis. ^{a, b}

Chapter No.	N-N	Peptide	Ru-peptide conjugates
Chapter 2		Ac- <u>H</u> RGD <u>H</u> -NH ₂	[Ru(bpy) ₂ (Ac-HRGDH-NH ₂)]Cl ₂
			[Ru(dmbpy) ₂ (Ac-HRGDH-NH ₂)]Cl ₂
			[Ru(Ph ₂ phen) ₂ (Ac-HRGDH-NH ₂)]Cl ₂
Chapter 3		Ac- <u>M</u> RGD <u>H</u> -NH ₂	Δ-[Ru(N-N) ₂ (Ac-MRGDH-NH ₂)]Cl ₂
		Ac- <u>M</u> RGD <u>H</u> -NH ₂	Λ-[Ru(N-N) ₂ (Ac-MRGDH-NH ₂)]Cl ₂
		Ac- <u>M</u> RVD <u>H</u> -NH ₂	Δ-[Ru(N-N) ₂ (Ac-MRVDH-NH ₂)]Cl ₂
		Ac- <u>M</u> RVD <u>H</u> -NH ₂	Λ-[Ru(N-N) ₂ (Ac-MRVDH-NH ₂)]Cl ₂
Chapter 4		Ac- <u>H</u> RGD <u>H</u> -NH ₂	Ru(Ph ₂ phen) ₂ (Ac-HRGDH-NH ₂)]Cl ₂
		Ac- <u>M</u> RGD <u>H</u> -NH ₂	Ru(Ph ₂ phen) ₂ (Ac-MRGDH-NH ₂)]Cl ₂
		Ac- <u>M</u> RGD <u>M</u> -NH ₂	Ru(Ph ₂ phen) ₂ (Ac-MRGDM-NH ₂)]Cl ₂
Chapter 5		Ac- <u>M</u> RGD <u>M</u> -NH ₂	Δ-[Ru(N-N) ₂ (Ac-MRGDM-NH ₂)]Cl ₂
		Ac- <u>m</u> rGd <u>m</u> -NH ₂	Λ-[Ru(N-N) ₂ (Ac-MRGDM-NH ₂)]Cl ₂
		Ac- <u>m</u> rGd <u>m</u> -NH ₂	Δ-[Ru(N-N) ₂ (Ac-mrGdm-NH ₂)]Cl ₂
		Ac- <u>M</u> rGd <u>M</u> -NH ₂	Λ-[Ru(N-N) ₂ (Ac-mrGdm-NH ₂)]Cl ₂
		Ac- <u>M</u> rGd <u>M</u> -NH ₂	Δ-[Ru(N-N) ₂ (Ac-MrGdM-NH ₂)]Cl ₂
			Λ-[Ru(N-N) ₂ (Ac-MrGdM-NH ₂)]Cl ₂

^a Coordinated amino acids are underlined. ^b L-amino acids are shown in uppercase letters, and D--amino acids are in lowercase.

1.7 References

1. Organization, W. H. Assessing national capacity for the prevention and control of noncommunicable diseases: report of the 2019 global survey. (2020).
2. X. Li, J. Kim, J. Yoon and X. Chen, *Advanced Materials*, 2017, **29**, 1606857.
3. S.-B. Yang, N. Banik, B. Han, D.-N. Lee and J. Park, *Pharmaceutics*, 2022, **14**, 1378.
4. S. Dilruba and G. V. Kalayda, *Cancer chemotherapy and pharmacology*, 2016, **77**, 1103-1124.
5. R. Oun, Y. E. Moussa and N. J. Wheate, *Dalton transactions*, 2018, **47**, 6645-6653.
6. C. R. R. Rocha, M. M. Silva, A. Quinet, J. B. Cabral-Neto and C. F. M. Menck, *Clinics*, 2018, **73**.
7. S. A. Aldossary, *Biomedical and Pharmacology Journal*, 2019, **12**, 7-15.
8. I. Ott, *Coordination Chemistry Reviews*, 2009, **253**, 1670-1681.
9. A.-R. Azzouzi, S. Vincendeau, E. Barret, A. Cicco, F. Kleinclaus, H. G. van der Poel, C. G. Stief, J. Rassweiler, G. Salomon and E. Solsona, *The Lancet Oncology*, 2017, **18**, 181-191.
10. G. Jaouen, A. Vessières and S. Top, *Chemical Society Reviews*, 2015, **44**, 8802-8817.
11. S. M. Meier-Menches, C. Gerner, W. Berger, C. G. Hartinger and B. K. Keppler, *Chemical Society Reviews*, 2018, **47**, 909-928.
12. A. Zamora, G. Viguera, V. Rodríguez, M. D. Santana and J. Ruiz, *Coordination Chemistry Reviews*, 2018, **360**, 34-76.
13. S. Campagna, F. Puntoriero, F. Nastasi, G. Bergamini and V. Balzani, in *Photochemistry and Photophysics of Coordination Compounds I*, Springer, 2007, pp. 117-214.
14. D. W. Thompson, A. Ito and T. J. Meyer, *Pure and Applied Chemistry*, 2013, **85**, 1257-1305.
15. M. Abrahamsson, H. Wolpher, O. Johansson, J. Larsson, M. Kritikos, L. Eriksson, P.-O. Norrby, J. Bergquist, L. Sun and B. Åkermark, *Inorganic chemistry*, 2005, **44**, 3215-3225.
16. L. Zayat, O. Filevich, L. M. Baraldo and R. Etchenique, *Phil. Trans. R. Soc. A*, 2013, **371**, 20120330.
17. H. Bregman, P. J. Carroll and E. Meggers, *Journal of the American Chemical Society*, 2006, **128**, 877-884.
18. F. E. Poynton, S. A. Bright, S. Blasco, D. C. Williams, J. M. Kelly and T. Gunnlaugsson, *Chemical Society Reviews*, 2017, **46**, 7706-7756.
19. A. Grzybowski, J. Sak and J. Pawlikowski, *Clinics in Dermatology*, 2016, **34**, 532-537.
20. B. C. Wilson and M. S. Patterson, *Physics in Medicine & Biology*, 2008, **53**, R61.
21. Z. Huang, H. Xu, A. D. Meyers, A. I. Musani, L. Wang, R. Tagg, A. B. Barqawi and Y. K. Chen, *Technology in cancer research & treatment*, 2008, **7**, 309-320.
22. W. Fan, P. Huang and X. Chen, *Chemical Society Reviews*, 2016, **45**, 6488-6519.
23. H. S. Jung, P. Verwilst, A. Sharma, J. Shin, J. L. Sessler and J. S. Kim, *Chemical Society Reviews*, 2018, **47**, 2280-2297.
24. Y. Chen, L. Bai, P. Zhang, H. Zhao and Q. Zhou, *Molecules*, 2021, **26**, 5679.
25. X. Li, J. F. Lovell, J. Yoon and X. Chen, *Nature Reviews Clinical Oncology*, 2020, **17**, 657-674.
26. G. M. F. Calixto, J. Bernegossi, L. M. De Freitas, C. R. Fontana and M. Chorilli, *Molecules*, 2016, **21**, 342.
27. J. P. Celli, B. Q. Spring, I. Rizvi, C. L. Evans, K. S. Samkoe, S. Verma, B. W. Pogue and T. Hasan, *Chemical reviews*, 2010, **110**, 2795-2838.
28. P. Agostinis, K. Berg, K. A. Cengel, T. H. Foster, A. W. Girotti, S. O. Gollnick, S. M. Hahn, M. R. Hamblin, A. Juzeniene and D. Kessel, *CA: a cancer journal for clinicians*, 2011, **61**, 250-281.
29. M. Triesscheijn, P. Baas, J. H. Schellens and F. A. Stewart, *The oncologist*, 2006, **11**, 1034-1044.
30. S. Bonnet, *Dalton Transactions*, 2018, **47**, 10330-10343.
31. K. Graham and E. Unger, *International journal of nanomedicine*, 2018, **13**, 6049.
32. P. Vaupel, M. Höckel and A. Mayer, *Antioxidants & redox signaling*, 2007, **9**, 1221-1236.
33. S. Monro, K. L. Colon, H. Yin, J. Roque III, P. Konda, S. Gujar, R. P. Thummel, L. Lilge, C. G. Cameron and S. A. McFarland, *Chemical reviews*, 2018, **119**, 797-828.
34. S. Chamberlain, H. D. Cole, J. Roque III, D. Bellnier, S. A. McFarland and G. Shafirstein, *Pharmaceutics*, 2020, **13**, 137.
35. S. Betanzos-Lara, L. Salassa, A. Habtemariam and P. J. Sadler, *Chemical communications*, 2009, 6622-6624.
36. Q.-X. Zhou, W.-H. Lei, Y.-J. Hou, Y.-J. Chen, C. Li, B.-W. Zhang and X.-S. Wang, *Dalton Transactions*, 2013, **42**, 2786-2791.
37. F. Barragán, P. López-Senín, L. Salassa, S. Betanzos-Lara, A. Habtemariam, V. Moreno, P. J. Sadler and V. Marchán, *Journal of the American Chemical Society*, 2011, **133**, 14098-14108.
38. L. N. Lameijer, D. Ernst, S. L. Hopkins, M. S. Meijer, S. H. Askes, S. E. Le Dévédec and S. Bonnet, *Angewandte Chemie*, 2017, **129**, 11707-11711.
39. V. H. van Rixel, V. Ramu, A. B. Auyeung, N. Beztsinna, D. Y. Leger, L. N. Lameijer, S. T. Hilt, S. E. Le Dévédec, T. Yildiz and T. Betancourt, *Journal of the American Chemical Society*, 2019, **141**, 18444-18454.
40. V. Van Rixel, B. Siewert, S. Hopkins, S. Askes, A. Busemann, M. Siegler and S. Bonnet, *Chemical science*, 2016, **7**, 4922-4929.
41. J.-A. Cuello-Garibo, M. S. Meijer and S. Bonnet, *Chemical Communications*, 2017, **53**, 6768-6771.
42. B. Siewert, V. H. van Rixel, E. J. van Rooden, S. L. Hopkins, M. J. Moester, F. Ariese, M. A. Siegler and S. Bonnet, *Chemistry—A European Journal*, 2016, **22**, 10960-10968.
43. L. N. Lameijer, S. L. Hopkins, T. G. Brevé, S. H. Askes and S. Bonnet, *Chemistry—A European Journal*, 2016, **22**, 18484-18491.

44. T. Sainuddin, J. McCain, M. Pinto, H. Yin, J. Gibson, M. Hetu and S. A. McFarland, *Inorganic Chemistry*, 2016, **55**, 83-95.
45. J. Hess, H. Huang, A. Kaiser, V. Pierroz, O. Blacque, H. Chao and G. Gasser, *Chemistry—A European Journal*, 2017, **23**, 9888-9896.
46. T. Sainuddin, M. Pinto, H. Yin, M. Hetu, J. Colpitts and S. A. McFarland, *Journal of Inorganic Biochemistry*, 2016, **158**, 45-54.
47. B. A. Albani, B. Peña, N. A. Leed, N. A. De Paula, C. Pavani, M. S. Baptista, K. R. Dunbar and C. Turro, *Journal of the American Chemical Society*, 2014, **136**, 17095-17101.
48. P. Kumar, S. Dasari and A. K. Patra, *European Journal of Medicinal Chemistry*, 2017, **136**, 52-62.
49. R. N. Garner, L. E. Joyce and C. Turro, *Inorganic Chemistry*, 2011, **50**, 4384-4391.
50. E. Wachter, D. K. Heidary, B. S. Howerton, S. Parkin and E. C. Glazer, *Chemical communications*, 2012, **48**, 9649-9651.
51. E. A. Medlycott and G. S. Hanan, *Chemical Society Reviews*, 2005, **34**, 133-142.
52. J. D. Knoll, B. A. Albani, C. B. Durr and C. Turro, *The Journal of Physical Chemistry A*, 2014, **118**, 10603-10610.
53. B. S. Howerton, D. K. Heidary and E. C. Glazer, *Journal of the American Chemical Society*, 2012, **134**, 8324-8327.
54. R. S. Becker, J. Seixas de Melo, A. L. Macanita and F. Elisei, *The Journal of Physical Chemistry*, 1996, **100**, 18683-18695.
55. Y. Chen, Y. Gao, Y. Li, K. Wang and J. Zhu, *Journal of Materials Chemistry B*, 2019, **7**, 460-468.
56. Z. Wang, R. Ma, L. Yan, X. Chen and G. Zhu, *Chemical communications*, 2015, **51**, 11587-11590.
57. M. Y. Nahabedian, R. A. Cohen, M. F. Contino, T. M. Terem, W. H. Wright, M. W. Berns and A. G. Wile, *JNCI: Journal of the National Cancer Institute*, 1988, **80**, 739-743.
58. J. F. Machado, J. D. Correia and T. S. Morais, *Molecules*, 2021, **26**, 3153.
59. T. Joshi, V. Pierroz, S. Ferrari and G. Gasser, *ChemMedChem*, 2014, **9**, 1419-1427.
60. J. C. Garrison, T. L. Rold, G. L. Sieckman, S. D. Figueroa, W. A. Volkert, S. S. Jurisson and T. J. Hoffman, *Journal of Nuclear Medicine*, 2007, **48**, 1327-1337.
61. J. Lee, D. G. Udugamasooriya, H.-S. Lim and T. Kodadek, *Nature chemical biology*, 2010, **6**, 258-260.
62. N. Curado, G. Dewaele-Le Roi, S. Poty, J. S. Lewis and M. Contel, *Chemical Communications*, 2019, **55**, 1394-1397.
63. S. Chakraborty, B. K. Agrawalla, A. Stumper, N. M. Vegi, S. Fischer, C. Reichardt, M. Kögler, B. Dietzek, M. Feuring-Buske and C. Buske, *Journal of the American Chemical Society*, 2017, **139**, 2512-2519.
64. P. Kaspler, S. Lazic, S. Forward, Y. Arenas, A. Mandel and L. Lilge, *Photochemical & Photobiological Sciences*, 2016, **15**, 481-495.
65. A. Gandioso, E. Shaili, A. Massaguer, G. Artigas, A. González-Cantó, J. A. Woods, P. J. Sadler and V. Marchán, *Chemical Communications*, 2015, **51**, 9169-9172.
66. A. Martin, A. Byrne, C. S. Burke, R. J. Forster and T. E. Keyes, *Journal of the American Chemical Society*, 2014, **136**, 15300-15309.
67. A. Byrne, C. S. Burke and T. E. Keyes, *Chemical science*, 2016, **7**, 6551-6562.
68. J. F. Machado, M. Machuqueiro, F. Marques, M. P. Robalo, M. F. M. Piedade, M. H. Garcia, J. D. Correia and T. S. Morais, *Dalton Transactions*, 2020, **49**, 5974-5987.
69. T. Wang, N. Zabarska, Y. Wu, M. Lamla, S. Fischer, K. Monczak, D. Y. Ng, S. Rau and T. Weil, *Chemical Communications*, 2015, **51**, 12552-12555.
70. S. Lien and H. B. Lowman, *Trends in biotechnology*, 2003, **21**, 556-562.
71. Y. Zheng, S. Ji, A. Czerwinski, F. Valenzuela, M. Pennington and S. Liu, *Bioconjugate chemistry*, 2014, **25**, 1925-1941.
72. A. G. Tkachenko, H. Xie, D. Coleman, W. Glomm, J. Ryan, M. F. Anderson, S. Franzen and D. L. Feldheim, *Journal of the American Chemical Society*, 2003, **125**, 4700-4701.
73. F. M. Veronese, *Biomaterials*, 2001, **22**, 405-417.
74. W. Tang and M. L. Becker, *Chemical Society Reviews*, 2014, **43**, 7013-7039.
75. L. M. De León-Rodríguez and Z. Kovacs, *Bioconjugate chemistry*, 2008, **19**, 391-402.
76. M. Langer, F. Kratz, B. Rothen-Rutishauser, H. Wunderli-Allenspach and A. G. Beck-Sickingler, *Journal of medicinal chemistry*, 2001, **44**, 1341-1348.
77. L. Blackmore, R. Moriarty, C. Dolan, K. Adamson, R. J. Forster, M. Devocelle and T. E. Keyes, *Chemical Communications*, 2013, **49**, 2658-2660.
78. C. Burke, A. Byrne and T. E. Keyes, *Journal of the American Chemical Society*, 2018, **140**.
79. C. S. Burke, A. Byrne and T. E. Keyes, *Angewandte Chemie*, 2018, **130**, 12600-12604.
80. K. S. Gkika, D. Cullinane and T. E. Keyes, *Metal Ligand Chromophores for Bioassays*, 2022, 27-74.
81. B. LaFoya, J. A. Munroe, A. Miyamoto, M. A. Detweiler, J. J. Crow, T. Gazdik and A. R. Albig, *International journal of molecular sciences*, 2018, **19**, 449.
82. S. J. Shattil, C. Kim and M. H. Ginsberg, *Nature reviews Molecular cell biology*, 2010, **11**, 288-300.
83. C. J. Avraamides, B. Garmy-Susini and J. A. Varner, *Nature Reviews Cancer*, 2008, **8**, 604-617.
84. P. EF, H. TA, Z. L, L. J and S. JW, *Journal of Biological Chemistry*, 2000, **275**, 21785-21788.
85. F. Danhier, A. Le Breton and V. r. Prêt, *Molecular pharmaceutics*, 2012, **9**, 2961-2973.
86. J. Bella and M. J. Humphries, *BMC structural biology*, 2005, **5**, 1-13.
87. M. Nagae, S. Re, E. Mihara, T. Nogi, Y. Sugita and J. Takagi, *Journal of Cell Biology*, 2012, **197**, 131-140.
88. S. Liu, *Molecular pharmaceutics*, 2006, **3**, 472-487.
89. R. J. Hatley, S. J. Macdonald, R. J. Slack, J. Le, S. B. Ludbrook and P. T. Lukey, *Angewandte Chemie International Edition*, 2018, **57**, 3298-3321.

90. J.-P. Xiong, T. Stehle, R. Zhang, A. Joachimiak, M. Frech, S. L. Goodman and M. A. Arnaout, *Science*, 2002, **296**, 151-155.
91. J. Zhu, B.-H. Luo, T. Xiao, C. Zhang, N. Nishida and T. A. Springer, *Molecular cell*, 2008, **32**, 849-861.
92. J. E. Harris, N. Desai, K. E. Seaver, R. T. Watson, N. A. Kane-Maguire and J. F. Wheeler, *Journal of Chromatography A*, 2001, **919**, 427-436.
93. N. A. Kane-Maguire and J. F. Wheeler, *Coordination Chemistry Reviews*, 2001, **211**, 145-162.
94. J. P. Schaeper, L. A. Nelsen, M. A. Shupe, B. J. Herbert, N. A. Kane-Maguire and J. F. Wheeler, *Electrophoresis*, 2003, **24**, 2704-2710.
95. P. Sun, A. Krishnan, A. Yadav, S. Singh, F. M. MacDonnell and D. W. Armstrong, *Inorganic chemistry*, 2007, **46**, 10312-10320.
96. F. Gasparrini, I. D'Acquarica, J. G. Vos, C. M. O'Connor and C. Villani, *Tetrahedron: Asymmetry*, 2000, **11**, 3535-3541.
97. D. W. Armstrong, Y. Tang, S. Chen, Y. Zhou, C. Bagwill and J.-R. Chen, *Analytical Chemistry*, 1994, **66**, 1473-1484.
98. P. Sun, A. Krishnan, A. Yadav, F. M. MacDonnell and D. W. Armstrong, *Journal of molecular structure*, 2008, **890**, 75-80.
99. X. Hua and A. G. Lappin, *Inorganic Chemistry*, 1995, **34**, 992-994.
100. J.-G. Liu, B.-H. Ye, Q.-L. Zhang, X.-H. Zou, Q.-X. Zhen, X. Tian and L.-N. Ji, *JBIC Journal of Biological Inorganic Chemistry*, 2000, **5**, 119-128.
101. Z. Lin, M. A. Celik, C. Fu, K. Harms, G. Frenking and E. Meggers, *Chemistry—A European Journal*, 2011, **17**, 12602-12605.
102. C. Fu, M. Wenzel, E. Treutlein, K. Harms and E. Meggers, *Inorganic Chemistry*, 2012, **51**, 10004-10011.
103. Z.-P. Zeng, Q. Wu, F.-Y. Sun, K.-D. Zheng and W.-J. Mei, *Inorganic Chemistry*, 2016, **55**, 5710-5718.
104. X. Li, A. K. Gorle, T. D. Ainsworth, K. Heimann, C. E. Woodward, J. G. Collins and F. R. Keene, *Dalton Transactions*, 2015, **44**, 3594-3603.
105. S. A. Funke and D. Willbold, *Molecular BioSystems*, 2009, **5**, 783-786.
106. A. Elfgen, M. Hupert, K. Bochinsky, M. Tusche, E. González de San Román Martín, I. Gering, S. Sacchi, L. Pollegioni, P. F. Huesgen and R. Hartmann, *Scientific reports*, 2019, **9**, 5715.
107. L. H. Leithold, N. Jiang, J. Post, T. Ziehm, E. Schartmann, J. Kutzsche, N. J. Shah, J. Breitreutz, K.-J. Langen and A. Willuweit, *Pharmaceutical research*, 2016, **33**, 328-336.
108. E. Hahn, N. Estrada-Ortiz, J. Han, V. F. Ferreira, T. Kapp, J. D. Correia, A. Casini and F. E. Kühn, *European Journal of Inorganic Chemistry*, 2017, **2017**, 1667-1672.
109. R. H. Holm, P. Kennepohl and E. I. Solomon, *Chemical reviews*, 1996, **96**, 2239-2314.
110. A. Iannello and A. Ahmad, *Cancer and Metastasis Reviews*, 2005, **24**, 487-499.
111. T. A. Waldmann, *Science*, 1991, **252**, 1657-1662.